

# Technical Notes

TECHNICAL NOTES are short manuscripts describing new developments or important results of a preliminary nature. These Notes cannot exceed 6 manuscript pages and 3 figures; a page of text may be substituted for a figure and vice versa. After informal review by the editors, they may be published within a few months of the date of receipt. Style requirements are the same as for regular contributions (see inside back cover).

## Extension of Inverse Design Techniques for Multicomponent Airfoils

M. Siladic\* and G. F. Carey†

University of Texas at Austin, Austin, Texas

### Introduction

FOR a given geometry of an airfoil section, potential flow analysis methods provide surface velocity and pressure distribution. For multicomponent airfoils, several practical design methods are based on surface singularity techniques: Bristow and Gross<sup>1</sup> introduce panel methods and demonstrate very efficient inverse and mixed analysis/design for single and multicomponent airfoils; Ormsbee and Chen<sup>2</sup> use a stream function method for multielement airfoil design, and Kennedy and Marsden<sup>3</sup> introduce an additional control point a finite distance from the trailing edge to satisfy the Kutta condition and reduce panel density. This method is also used as a starting solution in the design of single airfoils in viscous incompressible flow by Dutt and Srekanth<sup>4</sup> and for analysis and design of single airfoils in transonic flow by Greff and Mantel.<sup>5</sup> Conformal mapping techniques have been successfully applied by Halsey<sup>6</sup> and Saddhov and Hall<sup>7</sup> for analysis of multielement airfoils.

In the present work we use the stream function approach of Kennedy and Marsden.<sup>3</sup> In the design mode, however, we calculate the actual position of the trailing edge and then use linear interpolation to determine surface points. In this way it is possible to avoid generating saw-shaped airfoils that can result from the propagation of small errors due to selection of an additional trailing point as the actual trailing edge of the airfoil. The method is compared with several panel methods in representative application studies.

### Problem Formulation

As the normal velocity at a solid surface is zero, each solid surface is a streamline of the flow, and on the corresponding streamline,  $\psi$  is a constant. Thus, for a multiairfoil problem, the boundary conditions on an airfoil component  $k$  can be written as  $\psi = \psi_k$ . For a uniform stream incident at angle  $\alpha$  to the  $x$ -axis we have the boundary integral equation

$$\psi_k = y(S) \cos \alpha - x(S) \sin \alpha - \frac{1}{2\pi} \int_S \gamma(S') \ln[r(S, S')] ds' \quad (1)$$

where  $\psi_k$  is the unknown stream function on airfoil section  $k$ ,  $\gamma(S')$  is the vorticity strength at arbitrary point  $S'$ ,  $r(S, S')$  is the distance between points  $S$  and  $S'$ ,  $x(S)$ ,  $y(S)$  are

coordinates of the point of interest  $S$ , and  $s, s'$  are curvilinear coordinates measured along the airfoil surface starting at the trailing edge.

To solve Eq. (1), the airfoil surface is divided into  $N$  small surface elements, and the integral is approximated by summation of element contributions. For a general discussion see, e.g., Hess,<sup>8</sup> Brebbia,<sup>9</sup> and Carey and Kim.<sup>10</sup> Satisfying Eq. (1) at a control point  $C_i$ , we obtain

$$\psi_k + \sum_{j=1}^N \frac{1}{2\pi} \int_{S_j} \gamma(S_j) \ln[r(C_i, S_j)] ds_j = y_{C_i} \cos \alpha - x_{C_i} \sin \alpha \quad (2)$$

Selecting  $N$  control points  $C_i$ , the problem of potential flow over an airfoil section is reduced to that of solving these  $N$  simultaneous equations for  $\gamma_j = \gamma(S_j)$ .

The most immediate result of interest is the velocity distribution on the airfoil surface. Since the velocity inside the airfoil is zero, the discontinuity in tangential velocity across a vortex sheet is equal to the density of the vortex sheet. This implies that in solving Eq. (2) for  $\gamma_j$ , we directly obtain the velocity distribution on the airfoil surface.

In the present application of this method, we assume straight elements and a constant (or linear) distribution of  $\gamma_j$  over each element. On numerically evaluating the integrals in Eq. (2), we obtain the system

$$\psi_k + \sum_{j=1}^N \gamma_j K_{ij} = R_i \quad (i = 1, 2, \dots, N) \quad (3)$$

where  $K_{ij}$  is the influence coefficient of the element  $j$  for control point  $i$  and  $R_i$  is the right-hand side evaluated at control point  $i$ . The influence coefficients can be written as

$$K_{ij} = \int_{S_j}^{S_{j+1}} \ln[r(S_i, S_j)] ds \quad (4)$$

$M$  additional equations are determined using the Kutta condition for each airfoil section: for this purpose we use an additional control point at the extension of the bisector of the trailing edge and assume that the streamline through other control points passes through this point. Thus, with the Kutta condition enforced, Eq. (3) is expanded to include an additional  $M$  equations for the  $M$  airfoil sections:

$$\psi_k + \sum_{j=1}^N \gamma_j K_{Tj} = R_T \quad (5)$$

Only the right-hand side of the system of Eqs. (3-5) involves the angle of attack  $\alpha$ . Hence, if we want to determine flow at different angles of attack, it is necessary to determine coefficient matrix  $K_{ij}$  once only, and recalculate  $R_i$  as a function of the angle of attack. Solution of the system gives us an approximation to the nondimensional vortex density  $\gamma_j$  and the stream function  $\psi$ . The pressure coefficient on the airfoil surface may be obtained from the velocities via the equation

$$C_p(x_j, y_j) = 1 - (v_j/V_\infty)^2 = 1 - \gamma_j^2 \quad (6)$$

### Design Method

In an analysis mode, values of the surface coordinates  $x_i$ ,  $y_i$  are given so that the influence coefficients  $K_{ij}$  are uniquely defined by the airfoil geometry, and the system of Eq. (3) may be directly solved for the surface velocity distribution  $\gamma_j$ . However, for the airfoil inverse design problem, either values of surface velocities  $\gamma_j$  or pressure distribution are given a

Received Aug. 7, 1987; revision received Nov. 23, 1987. Copyright © American Institute of Aeronautics and Astronautics, Inc., 1988. All rights reserved.

\*Graduate Research Assistant, Department of Aerospace Engineering and Engineering Mechanics.

†Professor, Department of Aerospace Engineering and Engineering Mechanics.

priori, and an airfoil geometry  $(x_i, y_i)$  is to be determined. We approach this as an optimal control problem and apply an iterative procedure in which the geometry of a starting airfoil section is gradually modified until the desired velocity (pressure) distribution is achieved.

Substituting the desired values for stream function  $\psi^D$  and velocities  $\gamma_j^D$  in Eq. (3) while retaining  $K_{ij}$  from the previous design iteration allows solution for the geometry of a modified section. During the iteration process, the  $x_i$  coordinates are kept constant and new values of  $y_i$  calculated. For single-airfoil design, the value of airfoil stream function  $\psi$  is arbitrary, since its effect is only to move the airfoil up or down relative to the  $x-y$  coordinate system. However, in the case of multicomponent airfoils, the difference in stream functions between any two components determines the flow through the slot between the components, and specification of the stream function values depends on the type of design (i.e., given geometry of one or more sections, design the other components, or design all components).

To start the design process we define an admissible airfoil shape to generate the initial set of influence coefficients  $K_{ij}$ . The influence coefficients for each new iteration are then calculated using the coordinates obtained from the previous iteration. For example, at iteration  $m$  of the design procedure at the control points we have

$$y_i^m = \frac{1}{\cos \alpha} \left[ x_i \sin \alpha + \psi_k^R + \sum_{j=1}^N K_{ij}^{m-1} \gamma_j^R \right]; i = 1, 2, \dots, N \quad (7)$$

and at the trailing edge points,

$$y_T^m = \frac{1}{\cos \alpha} \left[ x_T \sin \alpha + \psi_k^R + \sum_{j=1}^N K_{ij}^{m-1} \gamma_j^R \right] \quad (8)$$

Since the location of the trailing point is very close to the trailing edge, we may assume that  $y_T$  is the location of the actual trailing edge. In this way, after each iteration we have the location of one point that determines the remaining points on the airfoil surface. The iteration process terminates if either of these conditions are met:

$$\max_i [ |y_i^m - y_i^{m-1}| ] \leq \tau_1 \quad (9)$$

or

$$\max_i [ |C_{pi}^m - C_{pi}^{m-1}| ] \leq \tau_2 \quad (10)$$

for tolerances  $\tau_1, \tau_2$ . As noted previously, during the design process the control points of the airfoils are adjusted along vertical lines  $x_i = \text{const}$ . This implies that there is no adjustment of coordinates parallel to the freestream direction. In practical applications this limitation may be relaxed because we have a prescribed chord length and can always employ an arbitrary  $x$  coordinate distribution.

The coordinates  $y_i$  that are obtained from Eqs. (7) and (8) are panel control points. Points on the airfoil surface can be determined by passing a curve through control points and interpolating or projecting a straight line through the control points using the trailing point as an actual trailing edge of an airfoil. In the latter method, however, a small error due to incorrect location of the trailing edge can propagate during iteration and produce a "saw-shaped" airfoil that can not satisfy the required pressure or velocity distribution. In order to avoid these difficulties, after each iteration we compute the actual position of the trailing edge using the first and last control points on the airfoil, the  $x$  coordinate of the trailing edge of the starting geometry, and the additional trailing point. In this way we can compute the coefficient matrix  $K_{ij}$  more accurately and use the actual trailing edge as a starting point for determination of the airfoil surface. For example, using the equation of a straight line through two points  $P_1$

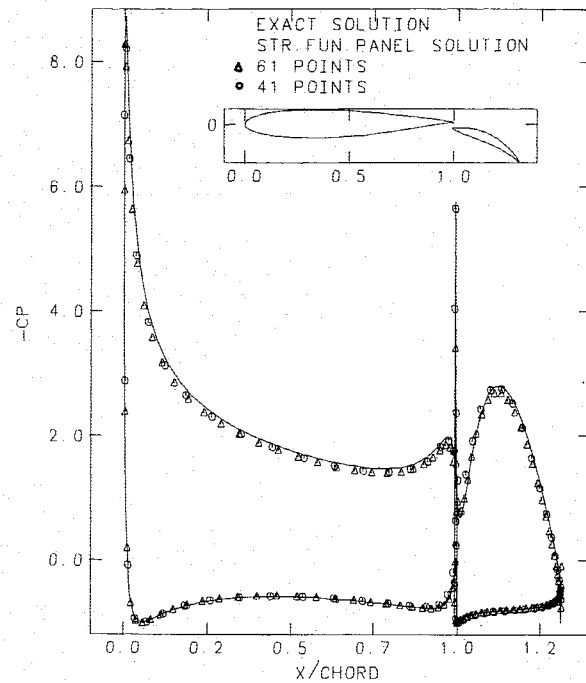


Fig. 1 Analysis computations for  $C_p$  of Williams' configuration.

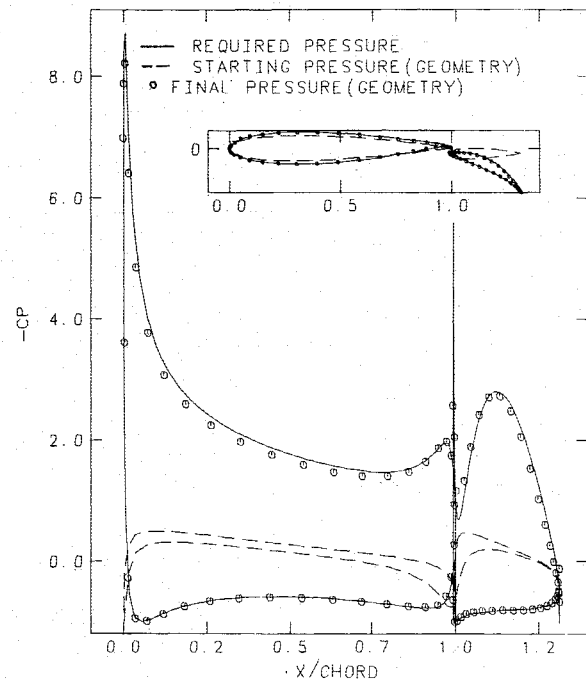


Fig. 2 Inverse design results to Williams' configuration from pair of NACA airfoils as starting configurations.

(the trailing edge) and  $C_1$  (the first control point), we can determine location of  $P_2$  (the second point on the airfoil surface), and so on.

## Results

### Airfoil Analysis

Example: Williams' Configuration at  $\alpha = 0$  deg (Fig. 1)

For analysis of multicomponent airfoils, a frequently studied test case is Williams' configuration with the flap at 10 or 30 deg. In the present example we use this configuration with the flap at 30 deg. The problem is solved with 41 and 60 panels on each section. The solution on the flap compares well with the exact solution, while on the lower surface of the main airfoil,

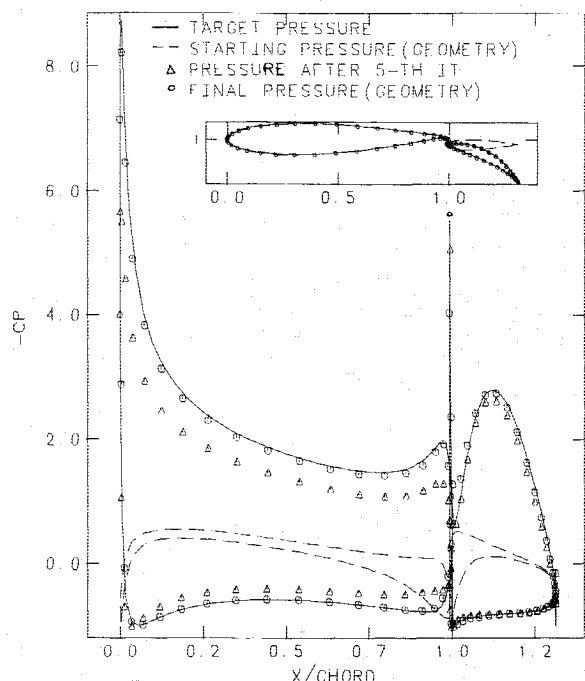


Fig. 3 Inverse design results to Williams' configuration with fixed main airfoil and initial NACA airfoil as flap.

there is a small difference between panel and exact solutions. The same problem is observed by Seeborn and Newman<sup>11</sup> using a linear vortex panel method with quadratic extrapolation of the Kutta condition. The present method gives approximately the same form of solution on the main airfoil but gives a better solution on the flap.

#### Airfoil Design

In multicomponent airfoil design, one may wish to consider 1) design of all components, 2) given main airfoil, design other components, and 3) given flap or slot, design of the main airfoil. The second case is the most interesting and practical because of several requirements that should be satisfied in design of high-lift devices. These requirements are 1) the flap and/or slot should retract to the main airfoil to form a good airfoil for cruising flight, 2) the deflection angles should provide reasonable increase of lift, and 3) the gap between the main section and the flap should provide enough energy to push the separation point of the boundary layer as much as possible toward the trailing edge of the flap.

**Example 1: Design of Williams' Configuration with Flap at 30 deg (Fig. 2)**

The required velocity distribution was taken from the exact solution at  $\alpha = 0$  deg. The starting geometry was composed from a NACA 0012 as main section and NACA 0009 as flap at zero angle of deflection. It is important that the algorithm not be sensitive to the initial flap angle and spacing, since these parameters are quickly adjusted by the design process. Since the  $x$  coordinates are not altered during the design process, the flap chord will change if the flap deflection is different from the starting deflection. For example, if a particular final flap chord is desired, we can determine an angle of deflection and set the starting flap at that angle.

The required surface velocities on both components were supplied together with stream functions  $\psi_1$  and  $\psi_2$  on the main section and flap, respectively. Discretization employed 80 elements—40 on each section. The design test case is very difficult because there is a high velocity peak at the leading edges of both sections. Very small deviation in coordinates of the leading edge will cause a change in pressure. It can be seen

that the pressure on the flap is very close to the required pressure distribution, and that at the leading edge of the flap the pressure peak is slightly overestimated. On the main section we have good agreement in pressure on the upper surface and at the leading and trailing edges but have underestimated pressure on the lower surface.

#### Example 2:

Here we design the same configuration as in the previous example but use the main William's airfoil and NACA 0009 as starting geometry (Fig. 3). That is, we want to design a flap with a fixed main airfoil. During the design process the velocity distribution on the main airfoil is assumed to be unknown and is replaced by the values computed in the previous iteration, while the geometry and location of the main section are held constant. It can be seen that after five iterations the pressure distribution on the flap is close to the required values, but there is a big difference in pressure distribution on the main section. The reason is a relatively slow change of pressure distribution on the flap. Final solution was obtained after nine iterations and gives good agreement with the pressure distribution in analysis mode.

#### Conclusion

Surface singularity methods are well suited to solution of potential flow problems in inverse design and can handle both single and multicomponent airfoils. The stream function approach and iterative control algorithm applied here appear to be numerically stable and applicable for practical airfoil design problems. The method provides accurate results in comparison with other surface singularity methods. For the cases studied, good results were obtained with 40–60 panels per airfoil section. The modified approach considered here for computing the actual position of the trailing edge provides designed airfoils with smooth shapes. The inverse design iteration was demonstrated to be efficient and stable for case studies of single and multi-component airfoils.

#### Acknowledgments

This research has been supported in part by AFOSR grant 87-0153.

#### References

- <sup>1</sup>Bristow, D. R. and Grose, G. G., "Development of Panel Methods for Subsonic Analysis and Design," NASA CR-3234, Feb. 1980.
- <sup>2</sup>Ormsbee, A. I. and Chen, A. W., "Multiple Element Airfoils Optimized for Maximum Lift Coefficient," *AIAA Journal*, Vol. 10, Dec. 1972, pp. 1620–1624.
- <sup>3</sup>Kennedy, J. L. and Marsden, D. J., "A Potential Flow Design Method for Multicomponent Airfoil Sections," *Journal of Aircraft*, Vol. 15, Jan. 1978, pp. 47–53.
- <sup>4</sup>Dutt, H. N. V. and Sreekanth, A. K., "Design of Airfoils for Prescribed Pressure Distribution in Viscous Incompressible Flows," *Aeronautical Quarterly*, Vol. 31, Part 1, Feb. 1980, pp. 42–55.
- <sup>5</sup>Greff, E. and Mantel, J., "An Engineering Approach to Inverse Transonic Wing Design Problem," *Communications in Applied Numerical Methods*, Vol. 2, Jan. 1986, pp. 47–56.
- <sup>6</sup>Halsey, N. D., "Potential Flow Analysis of Multielement Airfoils Using Conformal Mapping," *AIAA Journal*, Vol. 17, Dec. 1979, pp. 1281–1288.
- <sup>7</sup>Saddhoo, A. and Hall, I. M., "Test Cases for Plane Potential Flow Past Multi-Element Airfoils," *The Aeronautical Journal*, Vol. 89, No. 890, Dec. 1985, pp. 403–414.
- <sup>8</sup>Hess, J. L., "Improved Solution for Potential Flow About Arbitrary Axisymmetric Bodies by the Use of a Higher Order Surface Singularity Method," *Computer Methods in Applied Mechanics and Engineering*, Vol. 5, May 1975, pp. 297–308.
- <sup>9</sup>Brebbia, C. A., *Boundary Element Techniques in Engineering*, Pentech Press, London, 1978.
- <sup>10</sup>Carey, G. F. and Kim, S. W., "Lifting Aerofoil Calculation Using the Boundary Element Method," *International Journal for Numerical Methods in Fluids*, Vol. 3, Sept. 1983, pp. 481–492.
- <sup>11</sup>Seeborn, T. and Newman, B. G., "A Numerical Method for Calculating Viscous Flow Round Multiple-Section Airfoils," *Aeronautical Quarterly*, Vol. 26, Part 3, Aug. 1975, pp. 176–188.